Electronic structure, magnetic, and transport studies of single-crystalline $UCoGa_5$

R. Troć, Z. Bukowski, C. Sułkowski, and H. Misiorek
W. Trzebiatowski Institute of Low Temperature and Structure Research, Polish Academy of Sciences, 50-950 Wrocław, P. O. Box 1410, Poland

J. A. Morkowski and A. Szajek
Institute of Molecular Physics, Polish Academy of Sciences, 60-179 Poznań, uł. M. Smoluchowskiego 17, Poland

G. Chełkowska
A. Chełkowski Institute of Physics, Silesian University, 40-007 Katowice, uł. Uniwersytecka 4, Poland
(Received 16 December 2003; revised manuscript received 17 May 2004; published 30 November 2004)

The magnetic susceptibility, electrical resistivity in zero and in magnetic fields up to 8 T, thermopower and thermal conductivity measurements in a wide temperature range have been performed on $UCoGa_5$ single crystals. On the basis of the susceptibility maximum at 650 K and the phonon part of the thermal conductivity, a mixed-valence state of uranium in this compound has been postulated. On the other hand, a normal positive behavior of magnetoresistivity rules out the possibility of spin fluctuation as a mechanism driving the susceptibility through the maximum. In turn, the thermopower results may support both kinds of many-body behaviors. The electronic structure has also been studied by combining x-ray photoemission spectroscopy results with those obtained in the band structure calculations. In the latter the tight-binding linear muffin-tin orbital method in the atomic sphere approximation has been applied. A very good agreement between the experimental and calculated data has been achieved. A complex satellite structure of the core level spectra supports an idea of the presence of the valence instability in this compound. This idea is also concluded from the comparison of obtained experimental data with some similar rare earth and uranium ternary compounds.

DOI: 10.1103/PhysRevB.70.184443 PACS number(s): 71.20.Lp, 82.80.Pv, 72.15.−v

I. INTRODUCTION

The recent discovery of the Ce-based heavy fermion superconductors ($CeTIn_5$, T=Co, Rh, Ir)[1] and a fascinating new class of Pu-based superconductors ($PuTGa_5$, T=Co, Rh),[2,3] have clearly increased the interest in the 115-type compounds. This is especially true given a high transition temperature $T_s=18.5$ K found for $PuCoGa_5$ (Ref. 2). Much attention has also been focused on the physical properties of the uranium isomorphous ternaries $UTGa_5$, with T a transition metal. All of these materials adopt the $HoCoGa_5$-type structure.[4] This type of structure (s. g. P4/mmm) can be viewed as a uniaxially distorted UGa_3 unit cell with an additional TGa_2 layer put perpendicular to the [001] direction (*c* axis). From the c/a value of about 1.6 one can expect the quasi two-dimensional Fermi surface. In this structure the U and T atoms are located at the (1a) and (1b) positions, respectively. There are two positions for the Ga atoms at the (1c) and (4i) sites. The latter site has one free parameter *z*, which helps to determine the properties within the $UTGa_5$ series.[4] So compounds with *T*=Ni, Pd and Pt with average $z=0.313$ are magnetically ordered, while all the remaining members with $z\approx 0.305$, are not ordered to the lowest temperatures. The closest U-U distance in this family of $UTGa_5$ compounds is about 0.43 nm (being equal to the lattice parameter *a*). This is much larger than the so-called Hill limit,[5] whereby it has been suggested that in actinide compounds the 5*f* states become localized if the An-An spacing exceeds 0.34–0.35 nm. Despite this relatively large distance, previous polycrystalline[6–8] and recent single-crystalline magnetic studies[9] have shown that the 5*f* electrons in $UCoGa_5$ and other 1:1:5-type uranium intermetallics, have an itinerant character. For instance, the electronic heat capacity coefficient $\gamma(0)$ of 3.3–7 mJ/K^2 mol[8,9] for $UCoGa_5$ is as small as that of usual noble metals. There is no sign of heavy fermion behavior in this and in the other nonmagnetic isomorphic counterparts. As a reason for such a behavior, strong hybridization between the U 5*f* electrons and Ga 4*p* electrons has been assumed.[9] This is probably because as many as 12 gallium atoms are located in the first coordination sphere around the uranium atom, with only four other uranium atoms in the second sphere. Thus it may be that the 5*f* states can behave in a different way than one would expect on the basis of large An-An distances, so that, due to the *f*-electron hybridization with conduction and/or valence electrons, the phenomenon of valence fluctuation[10] takes place. For actinides this phenomenon has not been well documented. The mixed valence state of 5*f* electrons should be reflected predominantly in the dc magnetic susceptibility (a broad maximum), L_3-edge (two peak structure), photoemission spectra, e.g., for the -core lines (the distinct additional structure for f^n final states, corresponding to different *f* occupancies) and so on. A rapid promotion of the *f* electron from a narrow band to the conduction band and reverse is responsible for the nonmagnetic character of the compound despite the large atomic spaces. Hence the hybridization between the 5*f* and conduction states is considered to play a decisive role here.[11]

Evidence for the valence fluctuation behavior of uranium ions has been recently found for U_2Ru_2Sn.[12,13] The magnetic susceptibility of these ternaries has a maximum around 180 K which is characteristic of intermediate-valence behavior. The $\chi(T)$ data have been fitted to the interconfiguration

fluctuation model of Sales and Wohlleben[14] giving a value of $T_{sf}=155$ K for the characteristic fluctuation temperature. Due to the MV properties U_2Ru_2Sn shows typical Kondo semiconducting behavior.

In recent years, the electronic structure of $UCoGa_5$ has been intensively studied.[9,15] Mainly the relativistic linear augmented-plane wave (RLAPW) method in the local density approximation has been used in self-consistent calculations of the energy band structure. It appeared that all sheets of the Fermi surface (FS) are small in size and closed in topology. This makes $UCoGa_5$ a compensated semimetal, with small electron and hole FS.

A similar energy band structure is exhibited by $URhGa_5$ having the even number of electrons as $UCoGa_5$. On the other hand, the paramagnetic Fe- and antiferromagnetic Ni-, Pd- and Pt-containing gallides, having the odd number of electrons, form the large highly corrugated cylindrical Fermi surfaces along the tetragonal [001] direction. Such cylindrical FS's are formed also in $CeIrGa_5$ and $CeCoIn_5$ (Ref. 16).

A first account of our investigations of $UCoGa_5$ physical properties and its band structure has already been presented in a short conference paper.[17] We report here the detailed results of the magnetic, electronic and heat transport studies of the above compound together with the data of band structure calculations. They were based on the tight-binding linear muffin-tin orbitals method in the atomic sphere approximation, with spin orbit interactions included. Also the x-ray photoemission spectrum (XPS) of this ternary compound was measured and calculated with a satisfactory agreement.

II. EXPERIMENTAL

Single crystals of $UCoGa_5$ have been grown in two runs by the self-flux method. We used uranium and gallium from two sources with different purity. In the case of uranium the purity was 99.98% and 99.8%, whereas for gallium 99.99% and 99.9%. For both runs the purity of cobalt was the same, amounting to 99.98%. The elements were weighed in the atomic ratio of 1:1:15 and placed in an alumina crucible. The crucible was sealed in an evacuated silica tube and heated up to 1020°C for 24 h, followed by slow cooling (2–3°C/h) down to 600°C. After cooling to room temperature the still liquid flux was removed by decanting. Finally, thin film of Ga was etched away from single crystals by concentrated HCl. Single crystals of the title compound obtained in the two runs using lower and higher purity elements are denoted as samples I and II. Both grew in a form of platelets (up to 8 mm in size) with the *c* axis perpendicular to their surface.

The obtained crystals were examined using scanning electron microscopy and their composition was determined by means of energy dispersive x-ray microanalysis. The crystal structure was identified using single crystal x-ray diffraction. Practically we did not find any difference between I and II kind of single crystals. They have the same lattice parameters, as given for the sample I in our earlier paper.[17] Magnetization measurements were performed on oriented single crystals using a superconducting quantum interference device magnetometer within the temperature range of 4.2–800 K and in magnetic fields of 0.5 T. Electrical resistivity was measured employing a dc four-point technique. The current leads were soldered with a tin-lead alloy, while the voltage contacts were spot welded to the sample using short current pulses.

Thermoelectric power (TEP) measurements were carried on an oriented single crystal in the temperature range 8–300 K by a steady-state-mode semiautomatic instrument. The sample was clamped between two spring-loaded Cu blocks provided with heaters and a pair of Pt-1000's thermometers. The voltage difference between blocks was measured using a Keithley 181 Nanovoltmeter. The absolute TEP was obtained relative to the Seebeck coefficient of copper.

The thermal conductivity was measured by a steady-state method employing a manganin-constantan thermocouple and a small heater glued to the specimen. The temperature gradient along the sample was typically 0.3–0.4 K. Particular care was taken to avoid heat transfer between the sample and environment. The temperature distribution on the monel radiation shield was maintained close to the thermal gradient on the sample. The maximum experimental systematic error was below 3% (caused mainly by uncertainly in the sample geometry).

The x-ray photoelectron spectroscopy (XPS) spectra were obtained with monochromatized Al K_α radiation (1486.6 eV) at room temperature, using a PHI 5700/660 Physical Electronic Spectrometer. The energy spectra of the electrons were analyzed by a hemispherical mirror analyzer with an energy resolution about 0.3 eV. The Fermi level (E_F) was referred to gold for which the $4f$-level binding energy is 84.0 eV. All spectra were measured immediately after breaking the sample in vacuum of 5×10^{-10} Torr. To avoid oxygen contamination in the experimental chamber, the samples were repeatedly cleaved *in situ* about every 10 min. We did not observe any increase of the oxidation effect during the data acquisition time.

III. RESULTS AND DISCUSSION

A. Magnetic susceptibility

Magnetic molar dc susceptibility χ was measured up to the temperature of 800 K for two directions of magnetic field, $\mathbf{B}\|[100]$ (along the *a* axis) and $\mathbf{B}\|[001]$ (along the *c* axis). The obtained results are shown in Fig. 1 as the χ versus log *T* dependence. We have not observed a difference in susceptibility between crystals I and II, within an experimental error. There is an apparent anisotropy in the temperature runs of this quantity, where the $\mathbf{B}\|[100]$ configuration is less temperature dependent. The broad susceptibility maximum is seen at about 650 K, but more distinctly for the case where $\mathbf{B}\|c$ axis which could be indicative of magnetic fluctuation effects, probably playing a significant role in the magnetic behavior of $UCoGa_5$. As is also shown in this figure, the previous measurements made on the polycrystalline sample even up to above 1000 K have revealed similar results.[4] We have also plotted in this figure the data taken along the *a* axis at temperatures limited by 300 K and being recently obtained by Ikeda *et al.*[9] Furthermore, the susceptibility measurements carried on the samples being in poly-

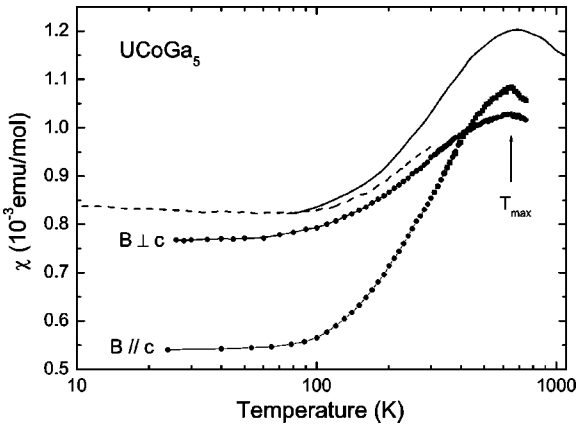

FIG. 1. Molar magnetic susceptibility χ vs log T measured in a field of 0.5 T along and perpendicular to the c axis. The solid line represents the data obtained by Grin, Rogl, and Hiebl,[4] while the dashed curve are data obtained by Ikeda *et al.*[9] on a single crystal of highest purity, where $B \| a$.

crystalline form but measured only in the temperature range up to 300 K[6–8] (not presented here) all show an increase in the susceptibility with increasing temperature. It turns out, that the susceptibilities of Rh-[4,9] and Ir-containing[18] 1:1:5 ternaries also behave in a similar way. This is in contrast, e.g., to the Fe-, Ru-, and Os-containing 1:1:5 ternaries,[4,19,20] the susceptibility of which decreases slightly when the temperature is increased. This fact presumably indicates that these ternaries having one 3*d* electron less do not behave as spin or valence fluctuators and represent rather typical metallic paramagnetism of a Pauli type.

B. Electrical resistivity

Figure 2 displays the electrical resistivity measured for the current $\boldsymbol{j}$ flowing parallel and perpendicular to the c axis for the sample II. Here one also sees the anisotropy in the transport properties, particularly in the shape of $\rho(T)$ dependencies. For both directions of the current the residual resistivity is rather high, especially for the $\boldsymbol{j} \| c$ case. Large values of ρ_0 were also reported for the polycrystalline samples.[6–8] Although the shapes of both curves are very similar to those measured by Ikeda *et al.*[9] on high purity single crystals, the difference in ρ_0 is about one order higher in magnitude for our single crystals. Hence, they could observe on their superpure crystals the de Haas–van Alphen effect determining the Fermi surface (FS) for $UCoGa_5$. It appears that the FS in this Co-containing compound consists of a small band 15-hole Fermi surface and a small band 16-electron Fermi surface. So that $UCoGa_5$ is a compensated semimetal with three kinds of ellipsoidal Fermi surfaces.

We have tried to make fitting of the Bloch–Grüneisen equation plus the band structure parameter KT^3 (Eq. (1)) into the experimental $\rho(T)$ data (solid lines).

$$\rho = \rho_0 + 4R\theta_D^R \left(\frac{T}{\theta_D^R}\right)^5 \int_0^{\theta_D^R/T} \frac{x^5 dx}{(e^x - 1)(1 - e^{-x})} + KT^3. \quad (1)$$

According to the Mott's theory,[21] the electron scattering on the *s*-*d* bands leads to this additional term in the description

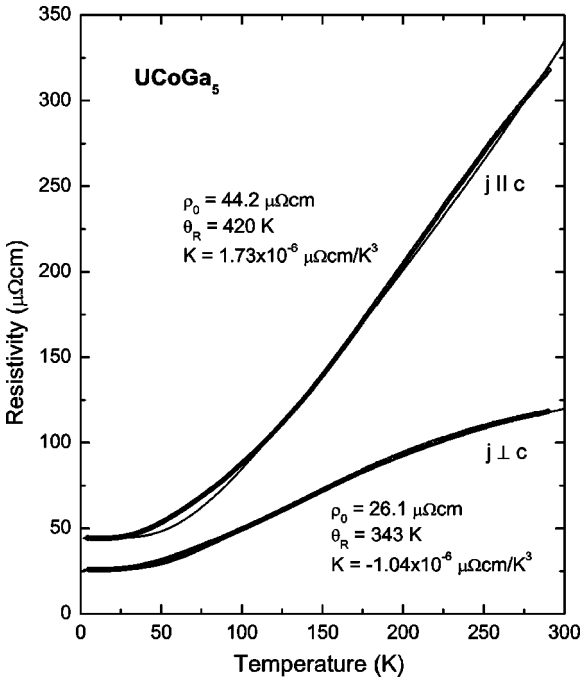

FIG. 2. Electrical resistivity ρ vs T measured for the current j parallel and perpendicular to the c axis. The displayed parameters were obtained by fitting of experimental results to the Bloch–Grüneisen equation (Eq. (1)).

of the temperature dependence of the resistivity of some transition metal alloys. The magnitude of constant K and its sign depend on the density of states at the Fermi level and its curvature. As seen in Fig. 2, there is a relatively good fitting only at higher temperatures for the case where $\boldsymbol{j} \| c$ axis. The somewhat better agreement in the whole range of temperatures is obtained for the $\boldsymbol{j} \perp c$-axis case. A similar result also along the a axis has been reported by Wawryk *et al.*[22] for $URhGa_5$. The Debye temperature obtained by us from the $\boldsymbol{j} \| a$-axis fitting curve having a value of 34 K is close to that reported by Ikeda *et al.*[9] being inferred from the heat capacity measurements ($\Theta_D = 370$ K).

In Fig. 3 the electrical resistivity as a function of squared temperature is presented. We note that at low temperatures there is distinctly seen a deviation from the Fermi liquid behavior. The $\rho(T)$ dependence for both current directions goes through a minimum at about 25 K confirming the earlier results reported by Noguchi and Okuda,[6–8] obtained by these authors on the polycrystalline samples. As different fittings of the $\rho(T)$ data to a T^n dependence showed, the T^2 variation is also followed for both directions of the current, but only in a small temperature range above about 90 K, as marked by the solid lines in Fig. 3. At low temperatures, below 90 K, we have satisfactorily fitted the higher power functions, e.g., with $n=4$ and 5 or only $n=4$ for the current directed either perpendicular or parallel to the c direction, respectively. The values of the obtained parameters are given in the figure. Thus, the above data have revealed a serious difference compared to the results reported for the very pure single-crystalline data of Ikeda *et al.*[9] The observed minimum in the resistivity can be understood to be a result of the competition of at least two contributions. One, ρ_k, is due to

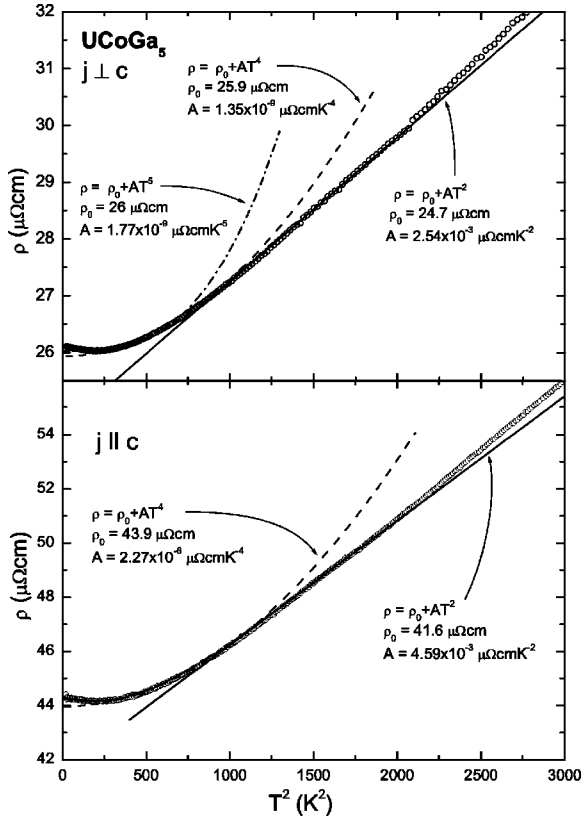

FIG. 3. Low temperature electrical resistivity ρ vs T^2 of sample II taken along and perpendicular to the c axis. The different fittings of the power functions to the experimental data with the obtained parameters are also displayed.

the electron scattering by the Kondo-type impurities or defects, the other one ρ_m is generated here by spin or valence fluctuations. The phonon contribution at so low temperatures can be negligible. By analogy with the situation existing for example in the case of single crystals of USb,[23] where such a minimum in $\rho(T)$ has been taken as the competition between the Kondo-type and antiferromagnetic spin-wave interactions, we have plotted in the inset to Fig. 4 the three $\rho_a(T)$ curves corresponding to the $\boldsymbol{j}\|a$ axis, obtained for the samples having different values of the residual resistivities. The residual resistivity ratio (RRR) values for these specimens cover a range between 2 and 61. Some rough outline of this Kondo-like resistivity component $\Delta\rho_k(T)$ can be obtained by subtracting the resistivity of the RRR=61 superpure sample[9] not exhibiting this effect from those of RRR =5 (II) and 2 (I) samples. In Fig. 4 there is shown in the reduced scale the dependence $\Delta\rho(T)/\Delta\rho$ (4.2 K) for these two cases I and II plotted versus log T. As seen, both these reduced temperature dependences are almost the same for these two cases. By taking this dependence as a Kondo-like, low temperature contribution to the total resistivity we could establish from the fitted Fermi-liquid relation: $\Delta\rho_k(T)/\Delta\rho$ (4.2 K)$[1-a(T/T_0)^n]$, where $n=2$ and T_0 =290 K, the Kondo temperature T_K, defined as being at $\Delta\rho_k(T)/\Delta\rho_k(0)=0.8$.[24] It was estimated to be 145 K, i.e., equal to $T_0/2$. Then, it becomes clear that even some small impurity contamination and/or atomic disorder as well as any

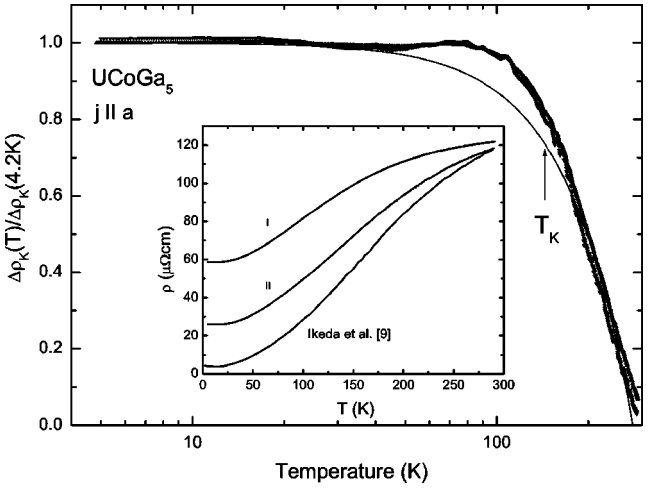

FIG. 4. The extracted Kondo-like behavior $\Delta\rho_K(T)/\Delta\rho_K$ (4.2 K) from the ρ vs T curves (inset) measured for $\boldsymbol{j}\|a$ for different purity samples I and II with RRR=2 and 5, respectively, compared to that with RRR=61 (Ref. 9). The solid line is a fitting of the above dependence to the equation: $\Delta\rho_K(T)$ $=\Delta\rho_K(4.2\text{ K})[1-a(T/T_0)^2]$, where $a=3\times10^{-3}$ and $T_0=290$ K.

defects may play in the case of $UCoGa_5$ a very important role in driving the system probably to the so-called nonmagnetic Kondo (NMK) effect, if it is not caused by any paramagnetic impurity ions (for an explanation of NMK effect see Ref. 25). Applying a similar procedure to the case $\boldsymbol{j}\|c$ failed due to an almost overall parallel shifting of all three corresponding $\rho(T)_c$ curves (not shown here). It seems that the difference in observed shape in $\rho(T)$, and overall magnitudes of the resistivity depending on the $\boldsymbol{j}$ direction (see Fig. 2), are generated, for example, by the anisotropy in hybridization of the $5f$ electrons with those of ligands, in the tetragonal unit cell. The full recognition of all these effects, however, can be achieved only by deep microscopic investigations, using neutron scattering, muon resonance or a large number of different spectroscopic-type methods.

The low temperature magnetoresistivity, defined as $\Delta\rho/\rho=[\rho(B)-\rho(0)]/\rho(0)$, as a function of magnetic field B applied perpendicular to the direction of the current $\boldsymbol{j}$ with strengths up to 8 T, measured for higher purity single crystals II is presented in Fig. 5 with the configurations given in the figure. One notes that the quadratic dependence aB^2 (solid lines) is fairly well obeyed at low temperatures for both directions of the current. Such a behavior may signal the existence of closed orbits on the FS in the **k** space if we deal with a compensated metal. The *dHvA* effect measured by Ikeda *et al.*[9] yields three kinds of *dHvA* branches, named a, b, and *c* which correspond to the closed orbits at the FS. All the surfaces are small in volume. This result classified $UCoGa_5$ to be a semimetal with equal volumes of electron and hole Fermi surfaces and very small value of the electron specific heat coefficient $\gamma(0)=3.3$ mJ/mol K^2.

As illustrated in Fig. 6, the temperature dependences of the magnetoresistivity have a similar shape and magnitudes for both directions of current, reaching at 4.2 K a rather high positive value of about 50% for $\boldsymbol{j}\|$ and $\boldsymbol{j}\perp$ to the c-axis directions, respectively. Moreover, one notes that even at

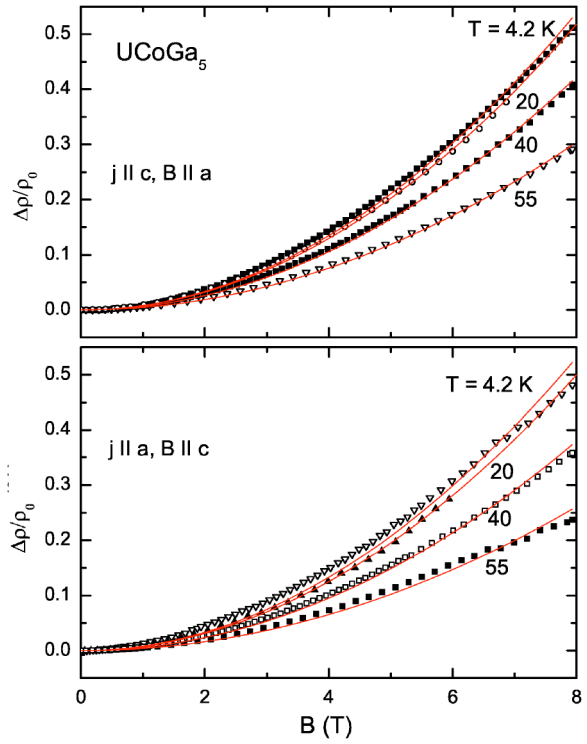

FIG. 5. Transversal magnetoresistivity $\Delta\rho/\rho_0$ vs B measured for the current $\boldsymbol{j}$ parallel and perpendicular to the c axis in magnetic fields up to 8 T, applied perpendicular to the $\boldsymbol{j}$-flowing direction. The results of fitting to the aB^2 behavior for both crystallographic directions are shown by the solid lines.

100 K the magnetoresistivity is still large amounting to about 10%. It is interesting to note that there is a lack, within the limit of experimental error, of any anisotropy in magnetoresistence (MR) and its temperature behavior is more reminiscent, e.g., of the nonspin fluctuator YAl_2 (about 30% at

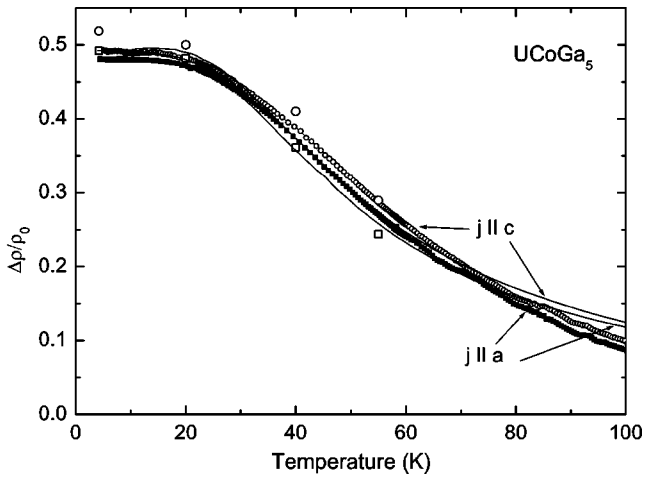

FIG. 6. Magnetoresistivity $\Delta\rho/\rho_0$ vs T measured along (open small circles) and perpendicular (filled small squares) to the c axis at 8 T. Both the open circles and squares are the data obtained from the $\Delta\rho/\rho_0$ vs B curves at 8 T (see Fig. 5). The magnetoresistance was LSQ-approximated (the solid lines) by the formula given by Eq. (2).

4.2 K and 8 T) than to YCo_2, representing the influence of the spin fluctuation (SF) scattering on MR.[26] The behavior of the former compound is considered as being caused by the only mechanism originating from the influence of the magnetic field on the conduction trajectories, the so-called Lorentz force effect, which always leads to an increase in the MR values towards low temperatures due to decreasing electron-phonon scattering. According to Gratz (see Ref. 27), this normal magnetoresistance can be approximated by the following formula:

$$\frac{\Delta\rho_{\perp}}{\rho} = \frac{B^2}{a[\rho(0,T)]_{a,c} + bB^2}, \tag{2}$$

where a and b are the field and temperature independent parameters depending on the conduction electron properties, established, for example, by the band structure at the Fermi level. $\rho(0,T)_{a,c}$ is the total resistivity in zero field for a given direction of the current. This is usually inferred in non-SF-type compounds from the Bloch–Grüneisen phonon relation, as that presented in Eq. (1) plus the residual resistivity ρ_0. The solid lines in Fig. 6 are the results of LSQ fit of Eq. (2) to the $UCoGa_5$ magnetoresistance data calculated for the two $\boldsymbol{j}$ directions, practically without difference in its temperature dependence. The fit parameters are: $a=8.76\ \mathrm{T}^2/\mu\Omega$ cm and $b=-4.03$ for parallel and $a=17.44\ \mathrm{T}^2/\mu\Omega$ cm and $b=-5.04$ for perpendicular direction of the current with respect to the c axis. The obtained results are then in contrast with the normal SF system, for which the growing negative magnetoresistance due to the suppression of SF by the magnetic field would be expected. Hence, the spin fluctuation effect signalized by the susceptibility maximum has not found any support from the magnetoresistivity data. Another possibility leading to the maximum at high temperatures in χ(T) is the valence fluctuation associated with the uranium atoms. This effect was considered as a reason for the maximum in the susceptibility, for example, in the Kondo-semimetal compound U_2Ru_2Sn.[13] However, one would expect some enhancement in the electronic heat coefficient, $\gamma(0)$, for both cases, i.e., for the spin-fluctuating and valence-instability materials. Nevertheless, for U_2Ru_2Sn this coefficient was found to be only 9 $\mathrm{mJ/K}^2$ mol U,[28] thus the value being comparable to that reported for $UCoGa_5$.

C. Thermoelectric power

Figure 7 shows the temperature dependence of the thermopower, S vs. T, for the temperature gradient applied along the parallel and perpendicular directions to the c axis. The same mechanism described above in the case of Mott's term in the electrical resistivity [see Eq. (1)] leads to the formula for the diffusion thermoelectric power of two-band conductor,[29] as is also the case, e.g., for $URhGa_5$.[22] The Mott two-band model for conduction and thermoelectric power usually gives reasonable estimates based on electronic structure data. As can be seen from Table II the density of states (DOS) at $E=E_F$ for s electrons, $N_s(E_F)$ is small as compared with $N_p(E_F)$, $N_d(E_F)$ and $N_f(E_F)$. If we assume, in the spirit of the Mott model, that the relaxation time $\tau_{s,pdf}$ for the conduction s electrons is due to their scattering into p, d and

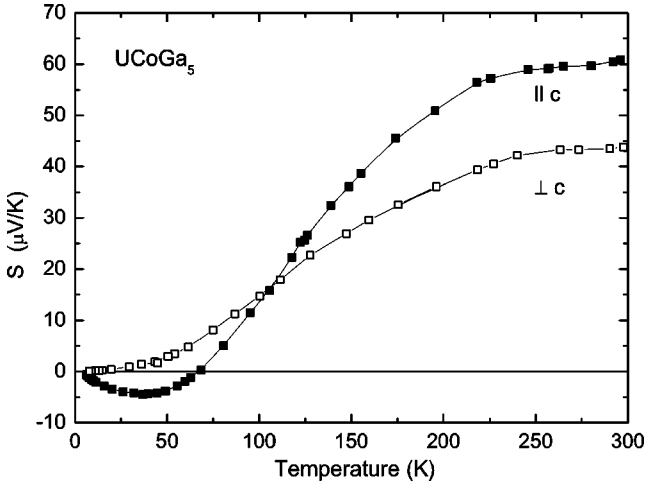

FIG. 7. Thermopower S vs T measured for the temperature gradient ΔT parallel and perpendicular to the c axis.

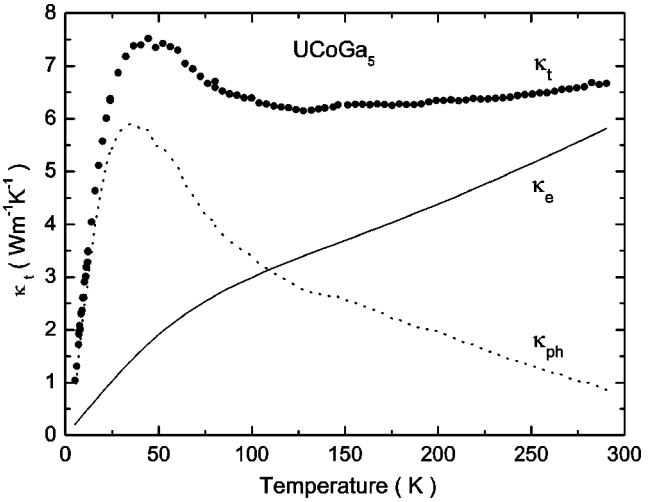

FIG. 8. Thermal conductivity κ_t vs T measured for the temperature gradient ΔT applied parallel to the a axis, κ_a.

f bands then $\tau_{s,pdf} \sim 1/N_{pdf}(E)$ where $N_{pdf}(E) = N_p(E) + N_d(E) + N_f(E)$. Since the conductivity of s electrons, σ_s, is proportional to $N_s(E)_{\tau s,pdf}$ it follows that $\sigma_s(E) \sim N_s(E)/N_{pdf}(E)$. From the standard expression for the thermopower

$$S \sim \left[\frac{\delta}{\delta E} \ln \sigma(E) \right]_{E_F} \tag{3}$$

one gets[29]

$$S_d(T) = \frac{\pi^2 k_B^2 T}{3e} \left\{ \left[\frac{1}{N_s(E)} \frac{dN_s(E)}{dE} \right]_{E=E_F} - \left[\frac{1}{N_{pdf}(E)} \frac{dN_{pdf}(E)}{dE} \right]_{E=E_F} \right\}. \tag{4}$$

Putting numbers from our band structure calculations we get from the formula (4) $S = 4.0 \cdot 10^{-2}(T/K)(\mu V/K) \cdot \mathrm{sign}(e)$. Assuming that holes are carriers of the current, positive sign of S is obtained. The order of magnitude of $|S|$ from this crude estimate is consistent with the data in Fig. 7. Except the diffusion term contribution into the total thermoelectric power, in general, there might be other ones caused by different mechanisms, as, for example S_{drag} (can be both of phonon and magnon origin) or S_{mb} associated with the many-body interactions in hybridized, strongly correlated electron bands of the Kondo- and spin-fluctuation (SF) or valence-fluctuation (VF) types.

It is interesting to note in the S vs T dependence that if the S_a measured along the a axis increases smoothly with temperature from zero to about 45 μV/K at room temperature, where S_a reaches a saturation, at the same time S_c measured along the c-axis first it goes through a negative minimum at 40 K and above about 75 K it becomes positive, also following saturation close to room temperature but with a relatively high value of 60 μV/K.

On the other hand, the VF compounds, like $CePd_3$, $CeSn_3$ and $CeIn_3$, exhibit large values of S at high temperature, but they have no extremum features at low temperatures.[30]

The large values of $S(T)$ (about 60 μV/K) and its mainly positive sign found in $UCoGa_5$ in two directions a and c in this paper as well as that in $URhGa_5$[22] along the a axis according to the Mott's formula [Eq. (4)] of diffusion thermopower first of all should be caused by a large magnitude of the energy derivative $dN_f(E)/dE$ at E_F. The reduced number of charge carriers and the low-characteristic temperature scales (1–100 K) of the systems, as is the case of strongly electron correlated ones, as a rule enhance the $S(T)$ to very large values.[31]

This is a rather common behavior in normal actinide intermetallic compounds, which do not show any signs of the presence of many-body effects, that the magnitude of the thermopower usually does not exceed 10–15 μV/K at room temperature (RT). This is supported, e.g., by the low S value of $ThCoGa_4$ reference compound amounting at RT to about 11 μV/K.[32] Only taking this fact into account it becomes apparent that so much enhanced values of the thermoelectric power in $UCoGa_5$ and $URhGa_5$ may also originate from some magnetic moment or valence instabilities existing in these compounds. Any better explanation of the thermopower behavior in such an intermetallic compound as $UCoGa_5$ will, however, require more investigations using a large variety of physical techniques.

D. Thermal conductivity

Figure 8 presents the temperature dependence of the thermal conductivity, $\kappa_t(T)$, measured along the temperature gradient ΔT applied parallel to the a axis, κ_a. This dependence shows a broad maximum in the vicinity of 50 K, a shallow minimum at 125 K and small linear increase with further increasing temperature. Almost the same $\kappa_t(T)$ variation was found for $\Delta T \| c$ axis, which indicates practically the lack of anisotropy in $\kappa_t(T)$. The total thermal conductivity being a sum of the electron and phonon contributions, $\kappa_t = (\kappa_e + \kappa_{ph})$ of the nonmagnetic material, but being characterized by the presence of the enhanced f-d electron hybridization, may be regarded as an inverse sum of three scattering mechanisms

responsible for the heat transport in a given metal if one assumes them to be additive (the Matthiessen rule). This can be expressed as follows:

$$\kappa_t = (W_{ph,i} + W_{ph,ph} + W_{ph,e})^{-1} + \kappa_e. \quad (5)$$

The particular terms in the bracket occurring in the above equation denote the thermal resistivities due to collisions of the phonons with lattice imperfections. The first term represents the scattering by point defect and impurities, the second term being the Umklapp ph-ph scattering and the third one is the phonon scattering on conduction electrons. In our case the latter one is the most important and is mainly connected to the possibility of the interactions in the material with some magnetic instabilities, like the spin (SF) or valence (VF) fluctuations. Another contribution involving the boundary scattering rate is important only at temperatures lower than 4.2 K and is not discussed here. A similar formula to that in bracket as in Eq. (5) can also be written for the electron heat component of the thermal conductivity, κ_e. All these different scattering contributions for both cases one might describe in terms of the proportionality to some simple power dependences T^n (see, e.g., Ref. 33). The scattering of electrons and phonons on the lattice imperfections is elastic and this mechanism is the most important at low temperatures. In contrast, the phonon-electron and phonon-phonon interactions may have an elastic as well as an inelastic character and they are described by processes of the normal and Umklapp types. In this case the scattering is exponentially dependent on the temperature.

Assuming as a first approximation the relation between the thermal conductivity and electrical resistivity, given by the Wiedemann–Franz law $\kappa_e\rho/T=L_0$ ($L_0=2.45\times10^{-8}$ W Ω K^{-2} is the Lorentz constant), we have derived the expected temperature variation of the electronic contribution, κ_e, to the total thermal conductivity using the electrical resistivity data obtained in this work. In turn, the phonon contribution we calculated from the difference: $\kappa_t-\kappa_e=\kappa_{ph}$. Consequently, in the figure together with the temperature dependence of the total κ_t along the a axis of $UCoGa_5$, also such dependencies of the corresponding contributions, i.e., the electronic κ_e and phonon κ_{ph} thermal conductivities were plotted. They are different not only in their magnitudes but also in the overall temperature changes. From these figures it is clear that above about 100 K, electrons mainly scatter on the conduction bands but below this temperature electrons scatter mainly on phonons. This leads to unusual behavior of $\kappa_{ph}(T)$ which goes through a pronounced peak at the vicinity of $T_{max}=40$ K and then it diminishes in a systematic way with a further increasing temperature. The reduction in $\kappa_{ph}(T)$ at temperatures above T_{max} is probably caused by the VF-ph interaction, known as being strong in the case of mixed-valent compounds.[34] Hence, in the first approximation, such a scattering, which becomes large for large values of the magnetic fluctuation temperature, may be regarded as being equivalent to the el-ph scattering (see, e.g., Ref. 35). Thus, one can treat the maximum in $\kappa_{ph}(T)$ as being the crossover from the el-ph scattering below T_{max} to the ph-ph scattering dominating above this temperature.

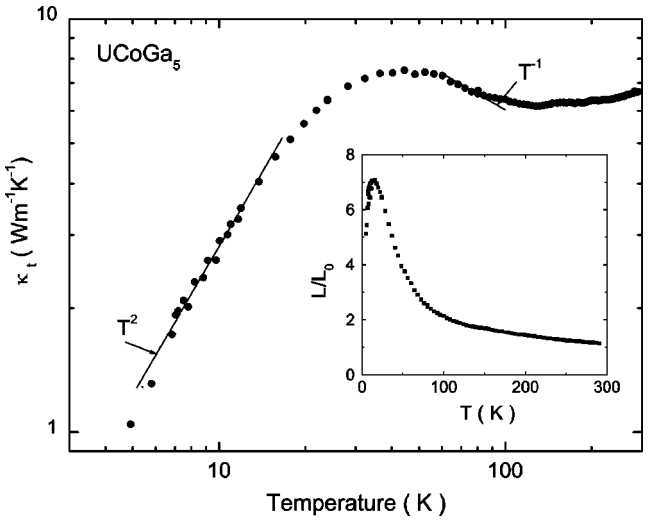

FIG. 9. Thermal conductivity κ vs T as in Fig. 8 but in the log-log scale. The straight lines represent T^2 and T^{-1} power laws as in the case of CeT(Sn, Sb), mixed-valence compounds, where T = Rh, Ni, Pt, presented in Fig. 3 of Ref. 35.

In Fig. 9 we have plotted the $\kappa_t(T)$ dependence in the log-log scale. The straight lines drawn below and above T_{max} show the T^2 and T^{-1} variations of $\kappa_t(T)$. The temperature squared dependence below T_{max} just shows that the el-ph mechanism is strongly favored at low temperatures. In the inset to this figure we present the reduced Lorenz L/L_0 number ratio versus temperature T. According to the domination of the phonon scattering at low temperatures this ratio is also enhanced by a factor of about 7 at about 20 K, where it goes through a sharp maximum. It should be mentioned that such an enhancement can be also caused by some inelastic ph-ph scattering of Umklapp type.[36] Only above about 100 K this ratio becomes close to 1 giving arguments for the validity of making the above analysis. On the other hand, we see from Fig. 8 that the electronic contribution goes through a very broad knee centered at about 50 K and then it falls down to zero at 0 K. Thus it manifests the importance of this type of scattering at higher temperatures. This behavior proves the well metallic conductivity character of $UCoGa_5$[9] which is responsible for a substantial electronic contribution κ_e to the measured κ_t. Exactly the same type of behavior has been inferred for well-known valence fluctuating compounds, such as CeT(Sn;Sb),[35] $Eu_3Pd_{20}Ge_6$,[37] and for some scutterudites.[38]

IV. ELECTRONIC BAND STRUCTURE AND XPS

The electronic band structure was calculated by the tight-binding linear muffin-tin orbital (LMTO) method in the atomic spheres approximation (ASA).[39] The room temperature experimental lattice parameters were used for computations, $a=0.42321$ nm, $c=0.67051$ nm.[17] Positions of atoms in the unit cell are provided in Table I. The electronic structure is calculated without spin polarization since the system is paramagnetic to the lowest temperatures studied. The unit cell contains one formula unit. In the ASA the unit cell is

TABLE I. Crystallographic characteristics for $UCoGa_5$: space group P4/mmm; lattice parameters $a=4.233$ Å, $c=6.723$ Å, average Wigner–Seitz radius 1.6016 Å.

Atom	Site	X_x	Y_y	Z_z	Wigner–Seitz radii [Å]
U	1a	0	0	0	1.9766
Co	1b	0	0	1/2	1.4890
Ga1	1c	1/2	1/2	0	1.6165
Ga2	4i	1/2	1/2	0.3048	1.5004

filled with the Wigner–Seitz (W–S) atomic muffin-tin spheres. Their radii are: 1.977, 1489, 1.616, and 1.500 Å for the U, Co, Ga(1c) and Ga(4i) atoms, respectively. The overlap volume is 12.6%. To compensate the ASA errors the standard combined corrections for overlapping W–S spheres were applied.[40] The exchange-correction potential was taken in the form proposed by Perdew *et al.*[41] The spin-orbit corrections were calculated according to the scheme of Min and Jang.[42] The scalar relativistic approximation for band electrons and the fully relativistic approach for core electrons were used.

The following initial atomic configurations were assumed: core$+6p^6 5f^3 6d^1 7s^2$ for U, core$+3d^7 4s^2$ for Co and core $+4s^2 4p^1$ for Ga. Computations were performed for 3927 k points in the irreducible wedge (1/16) of the Brillouin zone (B.Z.). Integrations in the B.Z. were made by the tetrahedron method.[43–45] Iterations were continued until the self-consistency of energy values was achieved within the error 0.01 mRy. From the computed partial densities of states (DOS) the valence band x-ray photoemission spectrum (XPS) was calculated by the standard procedure. The partial DOS-s weighted by the atomic cross sections for photon scattering[46] were convoluted with a Gaussian function to take into account a finite experimental resolution. The photon energy 1486.6 eV (Al K_α source) and the energy resolution $\delta=0.3$ eV were taken in accord with experimental parameters.

In the uppermost left hand panel of Fig. 10(a) the total DOS is presented, lower panels show the contributions from s, p, d and f electrons. Partial DOS's from U, Co and Ga (in two nonequivalent positions in the unit cell) are displayed in Figs. 10(a)–10(d), respectively. The most prominent features of the total DOS is the 1.3−eV-wide band from the U $5f$ electrons. The f band is split by about 0.7 eV due to the spin-orbit interactions. The Fermi level is situated in the valley between these two f subbands. A dip at E_F also appears for contributions from d and s electrons altogether giving rise to a remarkable dip at E_F in the total DOS. The band with a width of about 3 eV below E_F is a superposition of contributions from the d electrons, mainly from Co, and from p electrons, mainly provided by Ga. A striking feature is the very low value of partial DOS from the s electrons near E_F (see Table II). This property has presumably a strong effect on the transport properties of the system investigated here. In Table II the values of partial DOS at E_F are summarized. In turn the total numbers of states (NOS) are listed in Table III. A significant charge transfer from Ga to U and also to Co is indicative of a strong hybridization between the p, d and f states. As Fig. 5 indicates, no indication of the tendency to a saturation of the curves representing the magnetoresistance versus applied magnetic fields up to 8 T was found. The assumption of open orbits would be in disagreement with the recent calculations[15] of the Fermi surface for $UCoGa_5$. We have recalculated the Fermi surface using the code MSTUDIO, Princeton Technology Software 1998–2003. The obtained results appeared to be in good agreement with those reported in Ref. 15. Therefore, the results of the magnetic field dependence of the magnetoresistance can be understood in terms that $UCoGa_5$ has an even number of electrons per unit cell, and is a semimetal with the equal numbers of conduction electrons and holes, as was shown experimentally in Ref. 9.

TABLE II. DOS (E_F) $UCoGa_5$.

	U(1a)	Co(1b)	Ga(1c)	Ga2(4i)	Total (per f.u.)
s	0.002	0.003	0.026	0.011	0.075
p	0.009	0.025	0.207	0.083	0.573
d	0.128	0.359	0.034	0.008	0.553
f	2.937	⋯	⋯	⋯	2.937
Total	3.076	0.387	0.267	0.102	4.138

The valence band of the measured x-ray photoemission spectrum is presented in Fig. 11 and is compared with the calculated one (inset). The experimental curve contains raw data, no background subtracting has been applied. The agreement appears to be quite good, the observed features of the experimental curve have their counterparts in the calculated ones. In order to identify the role of the atomic ingredients in the spectrum the theoretical plot is decomposed into contributions from the U, Co and Ga atoms, respectively. The inset of Fig. 11 illustrates the different share to the XPS from the Ga atoms in the two nonequivalent crystallographic positions. Note that there are four times as many Ga atoms in the (4i) positions than in the (1c) ones. The lack of a distinct intensity enhancement at around −6 eV binding energy (BE), where the O($2s$) line usually appears, indicates that the sample practically is not contaminated by oxygen. The XPS in a broader BE range shows a strong narrow peak located at a BE of about −19 eV, originated from the Ga $3d$ core electrons. The calculated spectrum in this energy region is different, consisting of a weak peak at BE$=-19$ eV, but due to the U $6p$ core electrons and a strong peak from the Ga $3d$ core electrons, but located at a BE of about −15.5 eV. The discrepancy is apparently attributable to errors in the TB-LMTO method in this high-energy regime, as found also in other calculations (see, e.g., Ref. 47).

TABLE III. NOS (E_F) $UCoGa_5$.

	U(1a)	Co(1b)	Ga(1c)	Ga2(4i)	Total (per f.u.)
s	0.552	0.672	1.393	1.285	7.757
p	6.344	0.951	1.519	1.381	14.338
d	2.368	7.836	10.136	10.075	60.640
f	3.265	⋯	⋯	⋯	3.265
Total	12.529	9.459	13.048	12.741	86.000

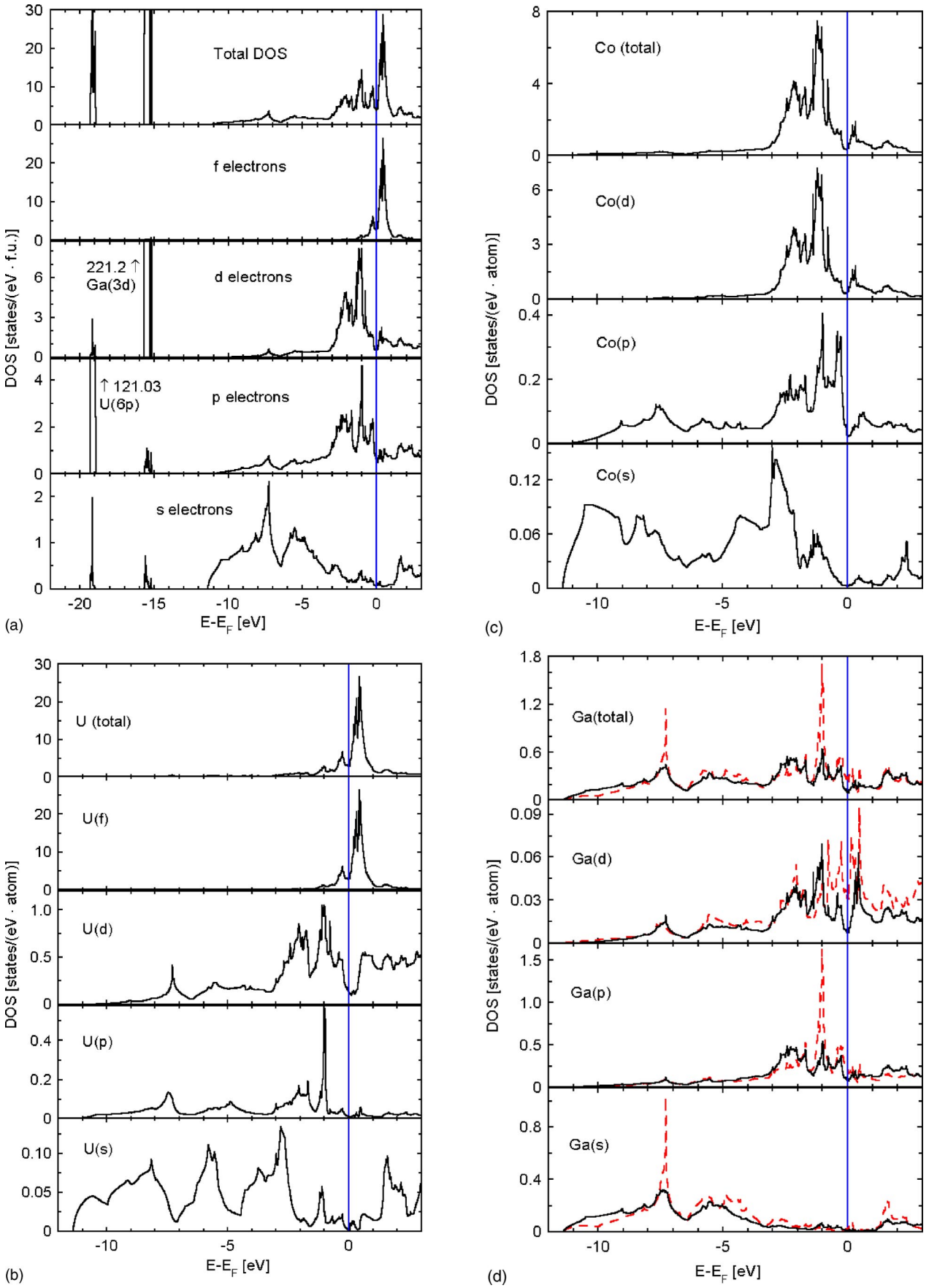

FIG. 10. Total and partial densities of states (a) and contribution to DOS from U (b), Co (c) and Ga (d). DOS's from Ga in the two nonequivalent positions are marked as the solid line for Ga(4i) and dotted line for Ga(1c), respectively.

Important information on the final states in the photoemission transitions can be extracted from the structure of the U $4f$ core lines. In the inset of Fig. 12 is shown the line U $4f$ split into $4f^{5/2}$ and $4f^{7/2}$ sublines by the spin-orbit interactions, separated by the typical splitting of about 11 eV. Unfortunately, in the present compound the structure of the U $4f^{5/2}$ peak is over covered by the nearby Ga *LMM* line (see the inset of Fig. 12). Therefore only the U $4f^{7/2}$ line can be unambiguously decomposed into the main line and its satellites. The decomposition was done by the standard procedure, as described in our earlier papers (see, e.g., Ref. 47). As seen from Fig. 12, there are, except for the main line, as many as two new satellites denoted in the figure as Nos. 1 and 2. The following values of the Doniach asymmetry parameters, α, were taken: 0.5 for the main line ($-$BE $=377$ eV), 0.3 for the satellite No. 1 (at 377.9 eV), and 0.03 for the satellite No. 2 (at 380.5 eV). Note that there is the lack of satellite No. 3, called 7 eV satellite, usually occurring in many uranium systems, having some localized character of their $5f$ electrons. This fact probably indicates an itinerant character at least of some part of $5f$ electrons in the compound studied. Satellite No. 2 at $-$BE$=380.5$ eV (so-called satellite -3 eV) is rather considered here as a result of the U^{4+} final state, as in the case of UO_2, than due to the problem of oxidizing the sample. However, we cannot exclude that this satellite is probably enhanced by a slight presence of uranium oxides, which just give a symmetric line near this position. Sample cleanness was checked by monitoring the oxygen and carbon ($1s$) levels. However, as the photoemission spectrum made in the whole energy range displays (Fig. 13), there is only a trace of the O($1s$) peak at $-$BE $=532$ eV (see the inset of Fig. 13). Along this line is also the fact that the intensity of this peak did not change even after 1.5 h lasting exposition of the sample during the measurements. Hence, one has to rule out the possibility of oxidizing the sample also during the time of experiment. Similar satellites, but around both main core lines of U $4f$, are also reported in other studies and are interpreted as being due to some mixed valence character of uranium with the $5f^2$ and

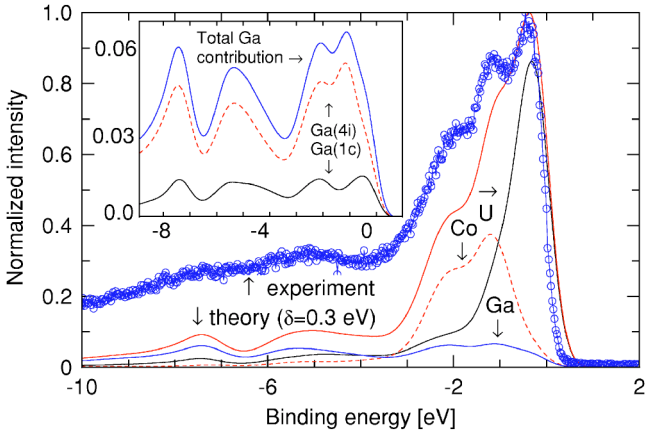

FIG. 11. The measured XPS for the valence band (the uppermost curve) compared with the calculated ones (the next curves from the top). The lines marked U, Co and Ga represent the respective contributions. The inset shows the contribution from the Ga atoms in the two nonequivalent sites, (4i) and (1c).

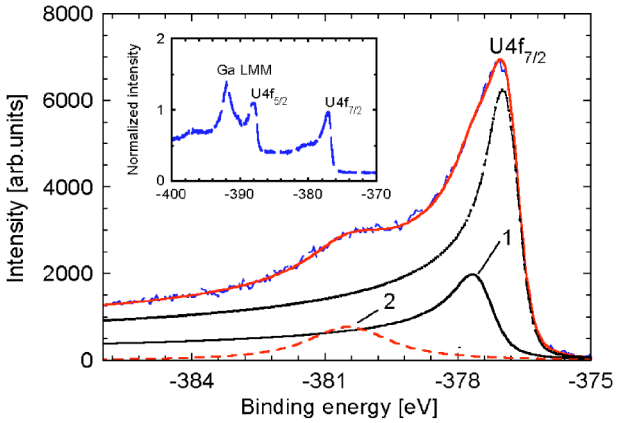

FIG. 12. The core line U $4f^{7/2}$ decomposed into the main line and two satellites denoted as Nos. 1 and 2. In the inset both components of the U $4f$ are shown.

$5f^3$ states (see, e.g., Refs. 47 and 48). In addition to the the 3 eV symmetric satellite described above we deal here also with the asymmetric one (No. 1) located at about 1 eV with higher BE than the main peak. We have observed such a satellite and studied the uranium ternary compound U_2Ru_2Sn, which has been established as being a mixed-valent compound and also classified as a semimetallic Kondo system.[49] Surprisingly, for this case no traces of the satellite No. 2 have been found. It is clear that this complex satellite structure in a number of ternary uranium compounds is attributed first of all with the initial ground electronic structure of uranium in these kinds of compounds. For better understanding of it more such studies are required.

V. CONCLUSIONS

We have performed a number of measurements such as the magnetoresistivity, thermopower and thermal conductivity on $UCoGa_5$ single crystals in order to study the effects of

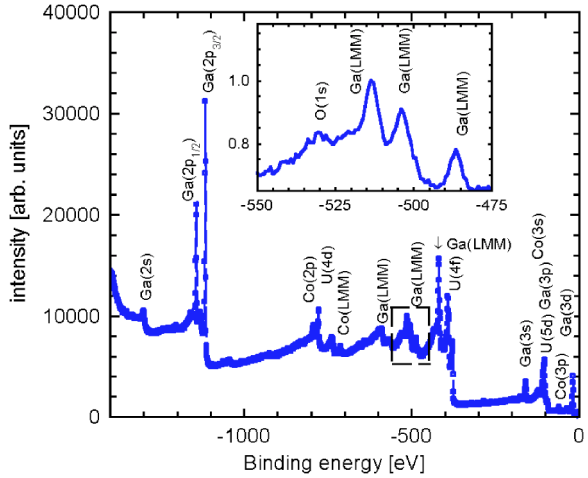

FIG. 13. The x-ray photoemission spectrum in the whole measured binding energy range. In the inset, on the extended scale, a weak peak indicating a trace amount of oxygen which eventually can be detected.

spin or valence fluctuations, the many-body phenomena which could be suggested by the presence of the susceptibility maximum at 650 K, observed in our earlier work.[17] First we found that the observed minimum in ρ(T) at 25 K and the dominant part of the remarkably high residual resistivity corresponds, at least along the $\boldsymbol{j} \| a$ axis, to the Kondo contribution, probably of nonmagnetic nature. The positive temperature variation of the MR measured at constant magnetic field of 8 T ruled out the distinct presence of spin fluctuations in the compound under study. The thermoelectric power depending on the measured direction could be explained by both types of instabilities in the crystal, depending on the temperature gradient direction. The temperature variation of the thermal conductivity favors the mixed-valence interpretation. Hence, it can be concluded that the uranium atoms in $UCoGa_5$ are probably in a mixed-valent state due to the substantial delocalization at least of some part of the $5f$ electrons by the extent $5f$-$4p$ hybridization acting in a somewhat similar way as in its parent compound UGa_3.[50] The only difference is that in the 1:1:5 case the unit cell of the the latter is enriched by an additional $CoGa_2$ layer. The good agreement of the valence bands found from XPS experiment and calculations gives further arguments for the almost itinerant character of the $5f$ electrons suitable here for the valence instability to occur. In addition, the complex $4f$ core photoemission spectra observed for $UCoGa_5$ very much supports this idea.

ACKNOWLEDGMENTS

The research was supported by the KBN Grant No. 2 P03B 024 22. The band structure computations were performed in the Supercomputer and Networking Center (PCSS) in Poznań.

[1] H. Shisido, R. Settai, A. Aoki, S. Ikeda, H. Nakawaki, N. Nakamura, T. Iizuka, Y. Inada, K. Sugiyama, and T. Takeuchi *et al.*, J. Phys. Soc. Jpn. **71**, 162 (2002).
[2] J. L. Sarrao, L. A. Morales, J. D. Thompson, B. L. Scott, G. R. Stewart, F. W. J. Rebizant, P. Boulet, E. Colineau, and G. H. Lander, Nature (London) **420**, 297 (2002).
[3] F. Wastin, P. Boulet, J. Rebizant, E. Colineau, and G. H. Lander, J. Phys.: Condens. Matter **15**, S2279 (2003).
[4] Y. Grin, P. Rogl, and K. Hiebl, J. Less-Common Met. **121**, 497 (1986).
[5] H. H. Hill, Nucl. Metall. **17**, 2 (1970).
[6] S. Noguchi and K. Okuda, J. Magn. Magn. Mater. **104–107**, 57 (1992).
[7] S. Noguchi and K. Okuda, Physica B **186–188**, 749 (1993).
[8] K. Okuda and S. Noguchi, *in Phys. Properties of Actinide and Rare Earth Compd.*, JJAP Series 8, 32 (1993).
[9] S. Ikeda, Y. Tokiwa, T. Okubo, Y. Haga, E. Yamamoto, Y. Inada, R. Seitai, and Y. Onuki, J. Nucl. Sci. Technol. **3**, 206 (2002); S. Ikeda, Y. Tokiwa, T. Okubo, M. Yamada, T. D. Matsuda, Y. Inada, R. Settai, E. Yamamoto, Y. Itaga, and Y. Onuki, Physica B **329–333**, 610 (2003).
[10] C. M. Varma, Rev. Mod. Phys. **48**, 219 (1976).
[11] J. M. Robinson, Phys. Rep. **51**, 1 (1979).
[12] P. de V. du Plessis, A. M. Strydom, and L. Menon, J. Phys.: Condens. Matter **13**, 8375 (2001).
[13] A. M. Strydom, and R. Troć, Solid State Commun. **126**, 207 (2003).
[14] B. C. Sales and D. K. Wohlleben, Phys. Rev. Lett. **35**, 1240 (1975).
[15] T. Maehira, M. Higuchi, and A. Hasegawa, J. Phys.: Condens. Matter **15**, S2237 (2003); T. Maehira, M. Higuchi, and A. Hasegawa, Physica B **329–333**, 574 (2003).
[16] Y. Onuki, R. Settai, K. Sugiyama, T. Takeuchi, T. C. Kobayashi, Y. Haga, and E. Yamamoto, J. Phys. Soc. Jpn. **73**, 769 (2004).
[17] J. Morkowski, A. Szajek, Z. Bukowski, C. Sułkowski, R. Troć, and G. Chełkowska, J. Magn. Magn. Mater. **272–276**, e323 (2004).
[18] V. Sechovský, L. Havela, G. Schaudy, G. Hilscher, N. Pillmayr, P. Rogl, and P. Fischer, J. Magn. Magn. Mater. **104–107**, 11 (1992).
[19] Y. Tokiwa, T. Maehira, S. Ikeda, Y. Haga, E. Yamamoto, A. Nakamura, Y. Onuki, M. Higuchi, and A. Hasegawa, J. Phys. Soc. Jpn. **70**, 2982 (2001).
[20] M. Schonert, S. Corsépius, E. W. Scheidt, and G. R. Stewart, J. Alloys Compd. **224**, 108 (1995).
[21] N. F. Mott, Proc. R. Soc. London, Ser. A **156**, 368 (1936).
[22] R. Wawryk, Z. Henkie, T. Cichorek, C. Geibel, and F. Steglich, Phys. Status Solidi B **232**, R4 (2002).
[23] R. Wawryk and Z. Henkie, Philos. Mag. B **81**, 223 (2001).
[24] M. B. Maple, R. P. Dickey, J. Herrmann, M. C. de Andrade, E. J. Freeman, D. A. Gajewski, and R. Chau, J. Phys.: Condens. Matter **8**, 9773 (1996).
[25] D. L. Cox and A. Zawadowski, Adv. Phys. **47**, 599R (1998); R. Wawryk, A. Wojakowski, C. Marucha, T. Cichorek, and Z. Henkie, Acta Phys. Pol. B **32**, 3487 (2001).
[26] E. Gratz, A. Lindbaum, A. S. Markosyan, and M. Milnera, J. Magn. Magn. Mater. **184**, 372 (1998); M. Coldea, D. Andreica, M. Bitu, and V. Crisan; *ibid.* **157–158**, 627 (1996).
[27] E. Gratz and A. S. Markosyan, J. Phys.: Condens. Matter **13**, R385 (2001).
[28] V. H. Tran, S. Paschen, N. S. A. Rabis, M. Baenitz, F. Steglich, P. dr V. du Plessis, and A. M. Strydom, Phys. Rev. B **67**, 075111 (2003).
[29] F. J. Blatt, P. A. Schroeder, C. L. Foiles, and D. Greig, *Thermoelectric Power of Metals* (Plenum, New York, 1976), p. 147.
[30] G. S. Garde and J. Ray, Phys. Rev. B **51**, 2960 (1995).
[31] E. Bauer, S. Berger, C. Paul, H. Michor, A. Grytsiv, and P. Rogl, Physica B **328**, 49 (2003).
[32] R. Wawryk, J. Stepień-Damm, Z. Henkie, T. Cichorek, and F. Steglich, J. Phys.: Condens. Matter **16**, 5427 (2004).
[33] J. M. Ziman, *Electrons and Phonons* (Oxford University Press, Oxford, 1960).
[34] J. M. Lawrence, P. S. Riseborough, and R. D. Parks, Rep. Prog. Phys. **44**, 1 (1981).
[35] J. Kitagawa, T. Sasakawa, T. Suemitsu, Y. Echizen, and T. Takabatake, Phys. Rev. B **66**, 224304 (2002).

[36] I. A. Smirnov and V. S. Oskotski, in *Handbook on the Physics and Chemistry of Rare Earths*, edited by K. A. Gschneidner, Jr. and L. Eyring (Elsevier, New York), p. 107.
[37] J. Kitagawa, T. Sasakawa, T. Suemitsu, T. Takabatake, and M. Ishikawa, J. Phys. Soc. Jpn. **71**, 1222 (2002).
[38] A. Gritsiv, P. Rogl, S. Berger, C. Paul, E. B. C. Godart, B. Ni, M. M. Abd-Elmeguid, A. Saccone, R. Ferro, and D. Kaczorowski, Phys. Rev. B **66**, 094411 (2002).
[39] G. Krier, O. Jepsen, A. Burkhardt, and O. K. Andersen, The TB-LMTO-ASA program (source code, version 4.7).
[40] O. K. Andersen, O. Jepsen, and M. Šob, *Electronic Structure and Its Applications* (Springer, Berlin, 1987).
[41] J. P. Perdew, J. A. Chevary, S. H. Vosko, K. A. Jackson, M. R. Pederson, D. J. Singh, and C. Fiolhais, Phys. Rev. B **46**, 6671 (1992).
[42] B. I. Min and J. R. Jang, J. Phys.: Condens. Matter **3**, 5131 (1991).
[43] O. Jepsen and O. K. Andersen, Solid State Commun. **9**, 1763 (1971).
[44] O. Jepsen and O. K. Andersen, Phys. Rev. B **29**, 5965 (1984).
[45] P. E. Blochl, O. Jepsen, and O. K. Andersen, Phys. Rev. B **49**, 16223 (1994).
[46] J. J. Yeh and I. Lindau, At. Data Nucl. Data Tables **32**, 1 (1985).
[47] G. Chełkowska, J. A. Morkowski, A. Szajek, and R. Troć, Phys. Rev. B **64**, 075119 (2001).
[48] S. Fujimori, Y. Saito, N. Sato, T. Komatsubara, S. Suzuki, S. Sato, and T. Ishii, J. Phys. Soc. Jpn. **67**, 4164 (1998).
[49] G. Chełkowska, J. A. Morkowski, A. Szajek, J. Stępień-Damm, and R. Troć, Eur. Phys. J. B **35**, 349 (2003).
[50] J. Rusz, M. Biasini, and A. Czopnik, Phys. Rev. Lett. **93**, 156405 (2004).